Cooper Pair Excitation Mediated by a Molecular Quantum Spin on a Superconducting Proximitized Gold Film

Stefano Trivini,[1,*] Jon Ortuzar,[1] Katerina Vaxevani,[1] Jingchen Li,[1,2] F. Sebastian Bergeret,[3,4] Miguel A. Cazalilla,[4,5,†] and Jose Ignacio Pascual[1,5,‡]

[1]*CIC nanoGUNE-BRTA, 20018 Donostia-San Sebastián, Spain*
[2]*School of Physics, Sun Yat-sen University, Guangzhou 510275, China*
[3]*Centro de Física de Materiales (CFM-MPC) Centro Mixto CSIC-UPV/EHU, E-20018 Donostia-San Sebastián, Spain*
[4]*Donostia International Physics Center (DIPC), 20018 Donostia-San Sebastian, Spain*
[5]*Ikerbasque, Basque Foundation for Science, 48013 Bilbao, Spain*

(Received 1 July 2022; accepted 17 February 2023; published 30 March 2023)

Breaking a correlated pair in a superconductor requires an even number of fermions providing at least twice the pairing energy Δ. Here, we show that a single tunneling electron can also excite a pair breaking excitation in a proximitized gold film in the presence of magnetic impurities. Combining scanning tunneling spectroscopy with theoretical modeling, we map the excitation spectrum of an Fe-porphyrin molecule on the Au/V(100) proximitized surface into a manifold of entangled Yu-Shiba-Rusinov and spin excitations. Pair excitations emerge in the tunneling spectra as peaks outside the spectral gap only in the strong coupling regime, where the presence of a bound quasiparticle in the ground state ensures the even fermion parity of the excitation. Our results unravel the quantum nature of magnetic impurities on superconductors and demonstrate that pair excitations unequivocally reveal the parity of the ground state.

DOI: 10.1103/PhysRevLett.130.136004

Superconducting materials are an ideal platform for designer quantum states with potential as qubits [1–3]. The superconducting ground state, a condensate of Cooper pairs, is protected from quasiparticle excitations by a pairing energy gap Δ. Ground state excitations can be achieved by electrons [4], correlated pairs in Josephson currents [5,6], or microwave photons [7–9]. In bulk superconductors, these excitations populate a continuum of Bogoliubov quasiparticles (QPs) and admix with other states that quickly quench their quantum coherence. Subgap quasiparticle excitations, in contrast, can live long in a coherent state. For example, sub-gap Andreev bound states in a proximitized link between two superconductors host addressable (doublet) QPs and (singlet) pair-breaking excitations with long quantum coherence [1,2]. QP states are odd in fermion parity and can be excited by adding a fermion to the even-parity BCS ground state [Fig. 1(a)]. Pair-breaking requires *two* correlated QPs into the pair-excited state, thus, with even parity [10]. Therefore, they are only accessible by absorption of one microwave photon or by addition of two fermions with opposite spin [Fig. 1(a)].

Subgap excited states can also appear when a magnetic impurity interacts with a superconductor via magnetic exchange J. These are the Yu-Shiba-Rusinov (YSR) [11–13] excitations, which are typically addressed by tunneling electrons from a scanning tunneling microscope (STM) [14–17]. YSR excitations correspond to the addition of a tunneling electron or hole into the ground state and appear in tunneling spectra as subgap bias-symmetric pairs of narrow peaks. In the regime of weak exchange interaction J, compared to the pairing energy Δ, YSR peaks are thus QP excitations of the BCS ground state. Pair excitations are, however, forbidden because these would require tunneling of two correlated electrons simultaneously [Fig. 1(b)].

Here, we report the observation of Cooper pair excitations in the YSR spectrum of an iron porphyrin molecule on a proximitized gold thin film. Owing to the magnetic anisotropy of the molecule, YSR states appear split in multiple resonances both inside and outside the proximitized gap. When the molecule lies in the Kondo-screened regime (J larger than Δ) pair excitations emerge as faint

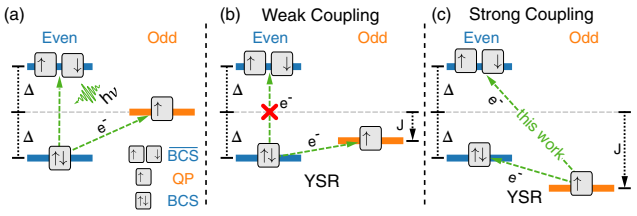

FIG. 1. (a) Scheme of the excitations of a superconductor with energy gap Δ. Pair excitations ($\overline{\mathrm{BCS}}$) can be probed by microwaves, while electrons can excite Bogoliubov quasiparticles. The arrow boxes refer to the number of quasiparticles involved. (b) The exchange J induces YSR bound states below Δ. Because of the parity selection rule single electrons cannot excite the pair excitation ($\overline{\mathrm{BCS}}$). (c) Increasing J, the ground state becomes odd in parity, and the $\overline{\mathrm{BCS}}$ state becomes accessible.

spectral resonances, scaling in energy with twice Δ. Supported by model calculations for quantum spins, we show that inducing pair excitations with single particles does not contradict parity-conservation rules when the magnetic molecule lies in the Kondo regime because the magnetic impurity is screened by a captured QP, turning the ground state odd in fermion parity [20–24]. From this ground state, single-particle tunneling allows now YSR excitations into even states such as the BCS state and its higher-lying pair-breaking excitation $\overline{\text{BCS}}$ [Fig. 1(c)].

Our measurements were performed at 1.2 K using to an STM (SPECS GmbH) under ultrahigh vacuum conditions. We used a V(100) single crystal as superconducting substrate ($T_c = 5.4$ K and $\Delta_V(1\,\text{K}) = 0.75$ meV). The clean V(100) surface appears with the characteristic (5×1) oxygen reconstruction [25,26], which does not affect its superconducting properties [27–31]. The V(100)-O(5×1) surface was covered with gold films, with thicknesses ranging from 1 to 10 ML, and shortly annealed to ~550 °C to produce epitaxial layers [Fig. 2(a)] with a 2.9 Å square lattice [inset Fig. 2(a)], compatible with an unreconstructed Au(100) surface [32,33], probably with some intermixing with the vanadium substrate [34].

The proximitization of the gold thin film was ascertained by comparing dI/dV spectra over the films and the bare V(100)-O(5×1) surface [Fig. 2(b)]. To enhance the spectral resolution we used superconducting tips obtained by tip indentations in the V(100) substrate. Spectra on V(100) show an absolute gap and two sharp peaks at $\pm(\Delta_t + \Delta_V)/e = \pm 1.5$ mV [Fig. 2(b)], corresponding to the convolution of superconducting density of states of tip (Δ_t) and sample ($\Delta_V/e = 0.75$ mV). Spectra on the investigated gold films also exhibit a similar hard gap [35], but with a pair of very sharp resonances at slightly smaller bias of $\pm(\Delta_s + \Delta_t)/e = 1.4$ mV. These peaks are attributed to QP excitations of de Gennes Saint-James (dGSJ) bound states in the gold film [36], which are Andreev pairs confined between the Au surface and the Au-V interface [Fig. 2(c)]. Owing to their confinement, the dGSJ QP excitation peaks shift to lower energy with increasing Au film thickness [37–41], and therefore are a useful knob for tuning the gap Δ_s in the experiment.

Next, we deposited the organometallic molecule iron tetraphenylporphyrin chloride (FeTPPCl) [Fig. 2(d)] on the proximitized gold films. This species hosts a Fe^{3+} ion with a $S = 5/2$ spin and easy plane magnetic anisotropy, which survives on metallic surfaces [42,43]. Some of the molecules retain the Cl ligand [Fig. 2(d)], and appear with two different shapes: the twofold symmetric FeTPPCl interact weakly with the substrate [41], while the fourfold symmetric molecules investigated here behave as quantum impurities coupled to the superconducting substrate.

Spectra on the fourfold FeTPPCl molecules are characterized by a complex pattern of intra and extragap resonances, as summarized in Fig. 2(e). Measuring with a superconducting tip, direct YSR resonances appear between $\pm\Delta_t$ and $\pm(\Delta_t + \Delta_s)$. We typically find three

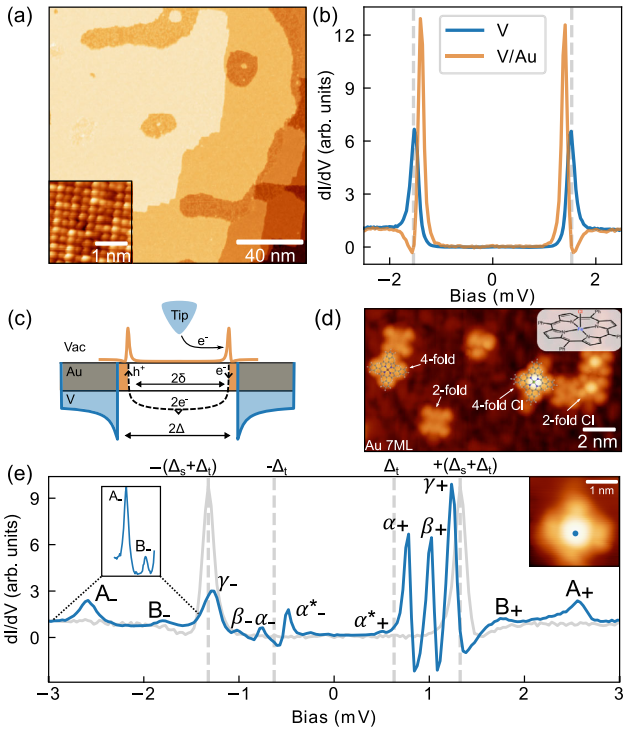

FIG. 2. (a) STM image of the epitaxial film produced by depositing 2 ML of Au on V(100) and annealing to 550 °C ($V_S = 10$ mV, $I = 100$ pA). Inset: constant height STM image of its square atomic lattice ($V_S = 10$ mV). (b) dI/dV spectra measured on V(100) and on Au/V. (c) Andreev reflections at the interface with V(100) deplete the film DOS and open a gap in the normal metal. (d) STM image showing different FeTPP and FeTPPCl species on 7 ML Au/V(100) ($V_S = 300$ mV, $I = 30$ pA), Inset: chemical structure of FeTPPCl. (e) dI/dV spectrum measured over a fourfold FeTPPCl molecule (in gray on the Au film), labeling two extragap states (A, B) and four intragap resonances $(\alpha, \alpha^*, \beta, \gamma)$. ($V_S = 3$ mV, $I = 75$ pA). Data analyzed with WSxM [18] and SpectraFox [19].

intragap pairs of peaks ($\alpha_\pm$, $\beta_\pm$, and $\gamma\pm$) that appear with larger intensity at positive bias due to finite potential scattering [44,45]. Additionally, the thermal YSR excitation $\alpha^*_\pm$ is observed below $\pm\Delta_t$ in the spectra.

In addition, dI/dV spectra show fainter peaks [$A_\pm$ and $B_\pm$ in Fig. 2(e)] above the proximitized gap. Since peak A lies at 1.3 meV above the gap-edge resonances, it can be associated with the $M_s = \pm 1/2 \rightarrow M_s = \pm 3/2$ spin-flip excitation of the molecular spin multiplet, with axial anisotropy constant $D = 0.65$ meV [41,42,46–48]. The origin of peak B, at ~0.6 meV outside the gap, cannot be directly connected with inelastic spin transitions. Instead, as shown in the following, peak B corresponds to a pair excitation of the superconducting condensate.

A hint on the origin of superconductors excitations can be obtained from their evolution with exchange coupling (J) variations [21–24,49]. In the tunneling regime, the STM tip exerts attractive forces that distort the *flexible* molecular system and reduce J. Moving the tip away from the

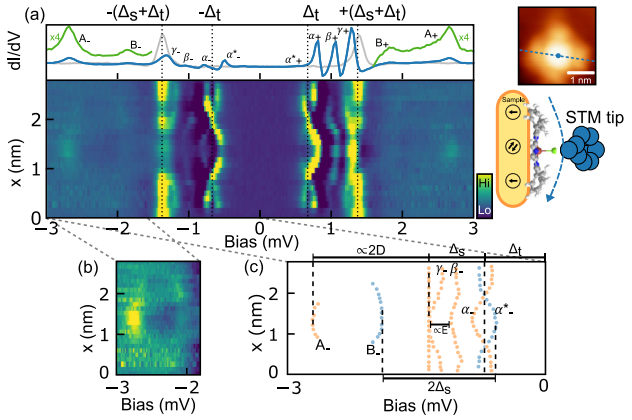

FIG. 3. (a) Map of dI/dV spectra measured across a fourfold FeTPPCl molecule (sketched on the right) with $V_S = 3$ mV and $I = 75$ pA. The spectrum on top is measured over the center. (b) Zoom of the extragap spectral region to highlight signals A and B. (c) Energy position of peaks at negative bias extracted from the line profile.

molecular center reduces this effect and causes an increase in J and a shift in dI/dV peaks. In the spectral map of Fig. 3(a), the three intragap YSR resonances shift to lower energies as the measuring position is laterally changed from the center towards the phenyl groups. For the α state the shift is large enough to cross the Δ_t line and exchange position with the thermal state α^*. This is a fingerprint of a parity-changing quantum phase transition (QPT) in the ground state of the molecule-superconductor system [21–23].

Unexpectedly, the extra-gap peaks A and B change intensity and position with J following different trends [Fig. 3(b)]: peak A vanishes towards the sides, while peak B, fainter in the center, shifts to higher energies. The apparent connection of the shifts of extra-gap peaks with intragap excitations [Fig. 3(c)] suggests they are all related to the same many-body state, renormalized by the tip-induced changes in J. This state is formed by the spin $S = 5/2$ of the quantum impurity, with $D \sim 0.65$ meV, coupled to the superconducting substrate with quasiparticle excitation peaks at Δ_s.

Theoretical model.—To interpret the results we used a minimal single-site model [50,51], extended for quantum impurities on superconductors by von Oppen and Franke [52,53]. Calculations using this model are light and provide useful insights into the many-body spectrum of the system. The Hamiltonian reads

$$\begin{aligned} H_s &= H_0 + H_M + H_J, \\ H_0 &= \Delta_s c_\uparrow^\dagger c_\downarrow^\dagger + \text{H.c.}, \\ H_M &= DS_z^2 + E(S_x^2 - S_y^2), \\ H_J &= \sum_{\sigma\sigma'} c_\sigma^\dagger [J_z S_z s_{\sigma\sigma'}^z + J_\perp (S_+ s_{\sigma\sigma'}^- + S_- s_{\sigma\sigma'}^+)] c_{\sigma'}, \end{aligned} \quad (1)$$

where H_0 describes a single-site superconductor, and H_M accounts for the magnetic impurity spin anisotropy, with transversal components E. The term H_J represents the (anisotropic) J between impurity and superconductor states characterized by J_z and $J_\perp$, axial and transverse exchange couplings, respectively.

In Fig. 4(a) we display the evolution with D and J of excitation energies in a tunneling experiment, obtained from the eigenstates of Eq. (1). Adding a tunneling electron (or hole) to the ground state of the system leads to a change in fermion parity. Therefore, only transitions between even and odd parity states are allowed [blue and orange in Fig. 4(a)]. For negligible exchange J, the molecular anisotropy D splits the spin multiplet into nondegenerate levels of equal S_z [left side in Fig. 4(a)]. The ground state is a product state of the molecular spin doublet and the BCS ground state

$$|\text{even}\rangle = |S_z\rangle \otimes |\text{BCS}\rangle = |\pm 1/2\rangle \otimes (|0\rangle + |2\rangle) \quad (2)$$

with $|0\rangle$ the vacuum and $|2\rangle = c_\uparrow^\dagger c_\downarrow^\dagger |0\rangle$. Tunneling experiments in this regime resolve peaks caused by a QP excitation at $\pm\Delta_s$, and by an additional spin excitation at $\pm(\Delta_s + 2D)$ [41,42,48]. The spin multiplet in the BCS ground state can also be thermally populated when $k_b T > 2D$ [22].

A finite exchange J [right panel in Fig. 4(a)] mixes the spin multiplet with Bogoliubov QPs into symmetric (+) and antisymmetric (−) entangled states with definite total

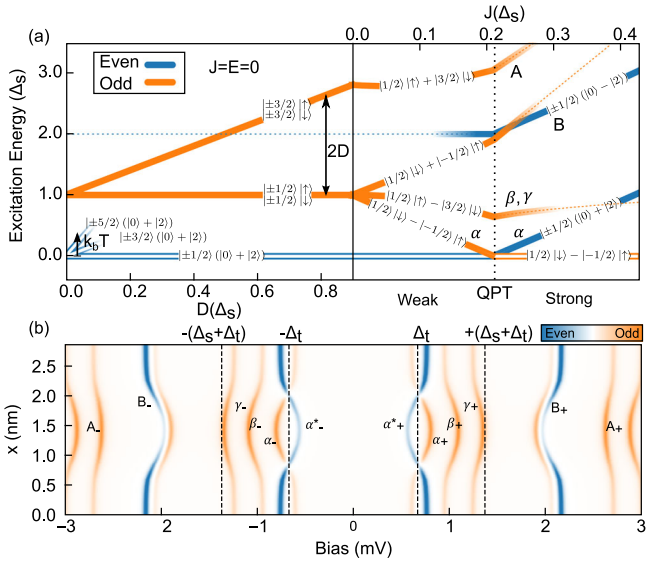

FIG. 4. (a) Allowed electron excitations, and their parity, for a spin 5/2 coupled to a superconductor, obtained from Eq. (1) Left: spin multiplet split by magnetic anisotropy D. Right: exchange coupling J leads to in-gap states. Around the QPT, thermal effects are shown as gradient lines. (b) Simulation of a spectral map like in Fig. 3(a) using the effective model, adopting as input the position of α and the re-normalized D ([54]).

spin projection S_z^T [55,56]. As shown in Fig. 4(a), *symmetric* states appear as excitations outside the gap, while the *antisymmetric* ones correspond to intragap excitations. For example, peak A in our experiments corresponds to the excitation of the entangled symmetric state with $S_z^T = 1$ [48], while the antisymmetric state is a YSR excitation split by the axial magnetic anisotropy [22,52,55,56]. In fact, resonances β and γ observed in the experiment are reproduced when a small transversal anisotropy E is also included to further split this state into two ([54]).

Increasing J above a critical value induces a QPT [Fig. 3(a)], where the ground state becomes an odd parity entangled state of impurity's spin and a QP [23,57]:

$$|\text{odd}\rangle = |1/2\rangle|\downarrow\rangle - |-1/2\rangle|\uparrow\rangle. \quad (3)$$

From $|\text{odd}\rangle$, there are two even parity states accessible by tunneling electrons or holes: the state (2), resulting in the YSR peaks α in spectra, and the state

$$\overline{|\text{even}\rangle} = |\pm 1/2\rangle \otimes \overline{|\text{BCS}\rangle} = |\pm 1/2\rangle \otimes (|0\rangle - |2\rangle). \quad (4)$$

This second state is a pair excitation, i.e., the excitation of two QPs over the BCS state: $\gamma_\uparrow^\dagger \gamma_\downarrow^\dagger |\text{BCS}\rangle = \overline{|\text{BCS}\rangle}$ [10,54,58]. The pair excitation lies at an energy $2\Delta_s$ above the YSR state, hence, it is independent of the molecular magnetic anisotropy [Fig. 5(a)]. As we discuss next, peak B in the spectra corresponds to this pair excitation.

In Fig. 4(b) we show a calculated spectral line profile simulating the experimental results of Fig. 3(a), obtained by solving the Hamiltonian (1). We obtain J from the position of α, $D = 0.65$ mV from measurements on weakly coupled molecules [41], and we include a small transversal anisotropy E that replicates β [54]. The results account for all excitations observed and reproduce their evolution with J, by using a single orbital channel. Fermion parity selection rules explain that peaks A, β, and γ fade away when the molecule enters in the strong interaction regime. Furthermore, the stronger intensity of peak B in this regime, and its shift with J agrees with the behavior of pair-excited state $\overline{\text{BCS}}$.

To further corroborate the identification of peak B as a pair excitation, we studied the evolution of peak A and B on 15 molecules lying on different regions and film thicknesses [Fig. 5(a)], with different values of Δ_s [Fig. 5(b)]. In these molecules, the position of peak B, measured with respect to α, scales with $2\Delta_s$ [Fig. 5(d)], as expected for pair excitations, ruling out other possible origins [59]. In contrast, the position of peak A with respect to Δ_s, i.e., $2D$, is uncorrelated from Δ_s [Fig. 5(c)].

The different evolution of peaks A and B with J is reflected by comparing spectra on the center of three molecules in different interaction regimes [Fig. 5(e)]. Peak A shifts to lower energy with increasing J, due to renormalization of D [48], and vanishes in the strong coupling case. Peak B, in contrast, becomes more intense in the strong coupling regime and shifts with J parallel to α, spaced by $2\Delta_s$, as expected for the pair excitation.

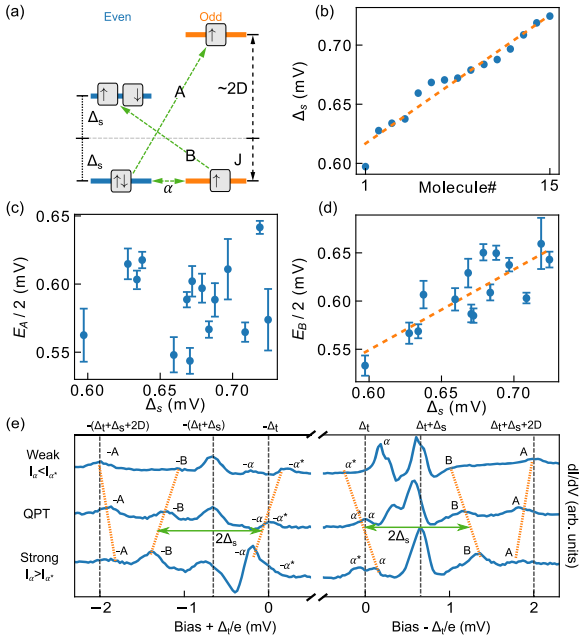

FIG. 5. a) Scheme of A and B excitations (J fixed to the QPT point); Peak A scales with anisotropy D and Peak B with Δ_s. (b) Value of Δ_s measured close to 15 different molecules lying on different positions on the substrate, and on films with different thicknesses. (c) Position of peak A for the 15 molecules, showing no correlation with Δ_s. (d) Evolution of peak B with Δ_s, showing a linear dependence. (e) Spectra of three molecules of the set, in weak, at QPT, and strong regimes (detected through the particle hole asymmetry of α). E_A is the energy of peak A over the gap edge, while E_B is the energy of peak B with respect to YSR state α. Peak A is more intense in the weak coupling case, while peak B in the strong coupling regime.

Discussion.—To date, pair excited states were only observed through adsorption of microwaves [1,2] photons, or Andreev pairs [6]. Fermion-parity conservation forbids a single tunneling electron from exciting a pair of Bogoliubov quasiparticles (the $\overline{\text{BCS}}$ state) in a superconductor. In our experiment, the observation of the pair excitation with electrons was made possible by the existence of an odd-parity Kondo-screened ground state of a magnetic molecule state on a superconductor, which enabled the excitation of two even-parity states [Fig. 3]: the BCS state, leading to the intra-gap YSR resonance and the $\overline{\text{BCS}}$ pair excited state, observed as peak B. Even if this resonance appears outside the spectral gap, the pair state in the proximitized film is a double population of a subgap state and, hence, it is expected to have a larger lifetime, facilitating its detection.

It is noteworthy that the quantum spin model used here accounted for all observed resonances using just one single channel. Multiple subgap excitations resulted by entangled

states of impurity and quasiparticles, mixed by magnetic anisotropy constants D and E. As we show in the Supplemental Material [54], a small value of E suffices to justify peak β, because the YSR excited state is integer and with large spin. This model successfully explains the important role of transversal and axial anisotropy and the effect of exchange on the magnetic anisotropy.

In conclusion, we have used a proximitized gold film as a platform for studying many-body excitations in magnetic impurities [35]. The magnetic molecule FeTPPCl interacting with the substrate electrons host subgap YSR states and spin excitations outside the gap that are readily described by a superposition of Bogoliubov quasiparticles and impurity spin states using a zero-bandwidth model. Interestingly, we found an excitation of a $\overline{\text{BCS}}$ pair state on molecules in the Kondo-screened regime, which scales with the different pairing energy of proximitized films of different thicknesses. This is an excitation that remains hidden to tunneling electrons and becomes available for magnetic impurities that bind a quasiparticle, thus behaving as a detector of the parity of the ground state. In a proximitized metal film, the excited pair populates dGSJ subgap states and inherits their coherent and spatial evolution and, thus, their potential for becoming elementary states for quantum processing.

We acknowledge financial support from Grants No. TED2021-130292B-C42, No. PID2019-107338RB-C61, No. CEX2020-001038-M, No. PID2020–112811 GB-I00, and Grant No. PID2020–114252 GB-I00, funded by MCIN/AEI/10.13039/501100011033, from the Diputación Foral de Guipuzcoa, and from the European Union (EU) through the Horizon 2020 FET-Open projects SPRING (No. 863098) and SUPERTED (No. 800923), and the European Regional Development Fund (ERDF). M. A. C. has been supported by Ikerbasque, Basque Foundation for Science, and MCIN Grant No. PID2020–120614 GB-I00 (ENACT). F. S. B. thanks Prof. Björn Trauzettel for his hospitality at Würzburg University, and the A. v. Humboldt Foundation for financial support. J. O. acknowledges the scholarship PRE_2021_1_0350 from the Basque Government.

*stefano.trivini@gmail.com
†miguel.cazalilla@gmail.com
‡ji.pascual@nanogune.eu

[1] C. Janvier, L. Tosi, L. Bretheau, Ç. Ö. Girit, M. Stern, P. Bertet, P. Joyez, D. Vion, D. Esteve, M. F. Goffman, H. Pothier, and C. Urbina, Science **349**, 1199 (2015).
[2] M. Hays, V. Fatemi, D. Bouman, J. Cerrillo, S. Diamond, K. Serniak, T. Connolly, P. Krogstrup, J. Nygård, A. L. Yeyati, A. Geresdi, and M. H. Devoret, Science **373**, 430 (2021).
[3] S. Park, W. Lee, S. Jang, Y.-B. Choi, J. Park, W. Jung, K. Watanabe, T. Taniguchi, G. Y. Cho, and G.-H. Lee, Nature (London) **603**, 421 (2022).
[4] I. Giaever, Phys. Rev. Lett. **5**, 464 (1960).
[5] A. MaassenvandenBrink, G. Schön, and L. J. Geerligs, Phys. Rev. Lett. **67**, 3030 (1991).
[6] L. Bretheau, Ç. Ö. Girit, H. Pothier, D. Esteve, and C. Urbina, Nature (London) **499**, 312 (2013).
[7] R. E. Glover and M. Tinkham, Phys. Rev. **104**, 844 (1956).
[8] F. J. Matute-Cañadas, C. Metzger, S. Park, L. Tosi, P. Krogstrup, J. Nygård, M. F. Goffman, C. Urbina, H. Pothier, and A. L. Yeyati, Phys. Rev. Lett. **128**, 197702 (2022).
[9] E. T. Mannila, P. Samuelsson, S. Simbierowicz, J. T. Peltonen, V. Vesterinen, L. Grönberg, J. Hassel, V. F. Maisi, and J. P. Pekola, Nat. Phys. **18**, 145 (2022).
[10] J. Bardeen, L. N. Cooper, and J. R. Schrieffer, Phys. Rev. **108**, 1175 (1957).
[11] L. Yu, Acta Phys. Sin. **21**, 75 (1965).
[12] H. Shiba, Prog. Theor. Phys. **40**, 435 (1968).
[13] A. I. Rusinov, Sov. J. Exp. Theor. Phys. **29**, 1101 (1969), http://jetp.ras.ru/cgi-bin/e/index/e/29/6/p1101?a=list.
[14] S.-H. Ji, T. Zhang, Y.-S. Fu, X. Chen, X.-C. Ma, J. Li, W.-H. Duan, J.-F. Jia, and Q.-K. Xue, Phys. Rev. Lett. **100**, 226801 (2008).
[15] B. W. Heinrich, J. I. Pascual, and K. J. Franke, Prog. Surf. Sci. **93**, 1 (2018).
[16] E. Cortés del Río, J. L. Lado, V. Cherkez, P. Mallet, J. Veuillen, J. C. Cuevas, J. M. Gómez Rodríguez, J. Fernández Rossier, and I. Brihuega, Adv. Mater. **33**, 2008113 (2021).
[17] L. Schneider, P. Beck, J. Neuhaus-Steinmetz, L. Róèsa, T. Posske, J. Wiebe, and R. Wiesendanger, Nat. Nanotechnol. **17**, 384 (2022).
[18] I. Horcas, R. Fernández, J. M. Gómez-Rodríguez, J. Colchero, J. Gómez-Herrero, and A. M. Baro, Rev. Sci. Instrum. **78**, 013705 (2007).
[19] M. Ruby, SoftwareX **5**, 31 (2016).
[20] T. Matsuura, Prog. Theor. Phys. **57**, 1823 (1977).
[21] K. J. Franke, G. Schulze, and J. I. Pascual, Science **332**, 940 (2011).
[22] N. Hatter, B. W. Heinrich, M. Ruby, J. I. Pascual, and K. J. Franke, Nat. Commun. **6**, 8988 (2015).
[23] L. Farinacci, G. Ahmadi, G. Reecht, M. Ruby, N. Bogdanoff, O. Peters, B. W. Heinrich, F. von Oppen, and K. J. Franke, Phys. Rev. Lett. **121**, 196803 (2018).
[24] L. Malavolti, M. Briganti, M. Hänze, G. Serrano, I. Cimatti, G. McMurtrie, E. Otero, P. Ohresser, F. Totti, M. Mannini, R. Sessoli, and S. Loth, Nano Lett. **18**, 7955 (2018).
[25] R. Koller, W. Bergermayer, G. Kresse, E. Hebenstreit, C. Konvicka, M. Schmid, R. Podloucky, and P. Varga, Surf. Sci. **480**, 11 (2001).
[26] F. Dulot, P. Turban, B. Kierren, J. Eugène, M. Alnot, and S. Andrieu, Surf. Sci. **473**, 172 (2001).
[27] M. Etzkorn, M. Eltschka, B. Jäck, C. R. Ast, and K. Kern, arXiv:1807.00646.
[28] H. Huang, J. Senkpiel, C. Padurariu, R. Drost, A. Villas, R. L. Klees, A. L. Yeyati, J. C. Cuevas, B. Kubala, J. Ankerhold, K. Kern, and C. R. Ast, Phys. Rev. Res. **3**, L032008 (2021).
[29] S. Karan, H. Huang, C. Padurariu, B. Kubala, A. Theiler, A. M. Black-Schaffer, G. Morrás, A. L. Yeyati, J. C. Cuevas,

J. Ankerhold, K. Kern, and C. R. Ast, Nat. Phys. **18**, 893 (2022).
[30] H. Huang, R. Drost, J. Senkpiel, C. Padurariu, B. Kubala, A. L. Yeyati, J. C. Cuevas, J. Ankerhold, K. Kern, and C. R. Ast, Commun. Phys. **3**, 199 (2020).
[31] H. Huang, C. Padurariu, J. Senkpiel, R. Drost, A. L. Yeyati, J. C. Cuevas, B. Kubala, J. Ankerhold, K. Kern, and C. R. Ast, Nat. Phys. **16**, 1227 (2020).
[32] R. Hammer, A. Sander, S. Forster, M. Kiel, K. Meinel, and W. Widdra, Phys. Rev. B **90**, 035446 (2014).
[33] Y.-F. Liew and G.-C. Wang, Surf. Sci. **227**, 190 (1990).
[34] E. Hüger, H. Wormeester, and K. Osuch, Surf. Sci. **580**, 173 (2005).
[35] J. O. Island, R. Gaudenzi, J. de Bruijckere, E. Burzurí, C. Franco, M. Mas-Torrent, C. Rovira, J. Veciana, T. M. Klapwijk, R. Aguado, and H. S. J. van der Zant, Phys. Rev. Lett. **118**, 117001 (2017).
[36] P. de Gennes and D. Saint-James, Phys. Lett. **4**, 151 (1963).
[37] G. B. Arnold, Phys. Rev. B **18**, 1076 (1978).
[38] E. Wolf and G. Arnold, Phys. Rep. **91**, 31 (1982).
[39] G. Kieselmann, Phys. Rev. B **35**, 6762 (1987).
[40] A. D. Truscott, R. C. Dynes, and L. F. Schneemeyer, Phys. Rev. Lett. **83**, 1014 (1999).
[41] K. Vaxevani, J. Li, S. Trivini, J. Ortuzar, D. Longo, D. Wang, and J. I. Pascual, Nano Lett. **22**, 6075 (2022).
[42] B. W. Heinrich, L. Braun, J. I. Pascual, and K. J. Franke, Nat. Phys. **9**, 765 (2013).
[43] B. W. Heinrich, L. Braun, J. I. Pascual, and K. J. Franke, Nano Lett. **15**, 4024 (2015).
[44] L. Farinacci, G. Ahmadi, M. Ruby, G. Reecht, B. W. Heinrich, C. Czekelius, F. von Oppen, and K. J. Franke, Phys. Rev. Lett. **125**, 256805 (2020).
[45] C. Rubio-Verdú, J. Zaldívar, R. Žitko, and J. I. Pascual, Phys. Rev. Lett. **126**, 017001 (2021).
[46] P. Berggren and J. Fransson, Europhys. Lett. **108**, 67009 (2014).
[47] P. Berggren and J. Fransson, Phys. Rev. B **91**, 205438 (2015).
[48] S. Kezilebieke, R. Žitko, M. Dvorak, T. Ojanen, and P. Liljeroth, Nano Lett. **19**, 4614 (2019).
[49] D. Chatzopoulos, D. Cho, K. M. Bastiaans, G. O. Steffensen, D. Bouwmeester, A. Akbari, G. Gu, J. Paaske, B. M. Andersen, and M. P. Allan, Nat. Commun. **12**, 298 (2021).
[50] I. Affleck, J.-S. Caux, and A. M. Zagoskin, Phys. Rev. B **62**, 1433 (2000).
[51] E. Vecino, A. Martín-Rodero, and A. LevyYeyati, Phys. Rev. B **68**, 035105 (2003).
[52] F. von Oppen and K. J. Franke, Phys. Rev. B **103**, 205424 (2021).
[53] H. Schmid, J. F. Steiner, K. J. Franke, and F. von Oppen, Phys. Rev. B **105**, 235406 (2022).
[54] See Supplemental Material at http://link.aps.org/supplemental/10.1103/PhysRevLett.130.136004 for details on the model and additional data.
[55] R. Žitko, R. Peters, and T. Pruschke, Phys. Rev. B **78**, 224404 (2008).
[56] R. Žitko, O. Bodensiek, and T. Pruschke, Phys. Rev. B **83**, 054512 (2011).
[57] A. V. Balatsky, I. Vekhter, and J.-X. Zhu, Rev. Mod. Phys. **78**, 373 (2006).
[58] M. Tinkham, *Introduction to Superconductivity*, 2nd ed. (Dover Publications, New York, 2004).
[59] J. Homberg, A. Weismann, T. Markussen, and R. Berndt, Phys. Rev. Lett. **129**, 116801 (2022).